



LAWRENCE
LIVERMORE
NATIONAL
LABORATORY

Fast Ignition relevant study of the flux of high intensity laser generated electrons via a hollow cone into a laser-imploded plasma

M.H. Key, J.C. Adam, K.U. Akli, M. Borgheshi, M.H. Chen, R.G. Evans, R.R. Freeman, S.P. Hatchett, J.M. Hill, A. Heron, J.A. King, K.L. Lancaster, A.J. Mackinnon, P.A. Norreys, T. Phillips, L. Romagnani, R. Snavely, R. Stephens, C. Stoeckl, R.Town, B. Zhang, M. Zepf

October 20, 2005

Physics of Plasmas

Disclaimer

This document was prepared as an account of work sponsored by an agency of the United States government. Neither the United States government nor Lawrence Livermore National Security, LLC, nor any of their employees makes any warranty, expressed or implied, or assumes any legal liability or responsibility for the accuracy, completeness, or usefulness of any information, apparatus, product, or process disclosed, or represents that its use would not infringe privately owned rights. Reference herein to any specific commercial product, process, or service by trade name, trademark, manufacturer, or otherwise does not necessarily constitute or imply its endorsement, recommendation, or favoring by the United States government or Lawrence Livermore National Security, LLC. The views and opinions of authors expressed herein do not necessarily state or reflect those of the United States government or Lawrence Livermore National Security, LLC, and shall not be used for advertising or product endorsement purposes.

Fast ignition relevant study of the flux of high intensity laser generated electrons via a hollow cone into a laser-imploded plasma

M.H. Key¹, J C Adam⁹, K.U. Akli¹, M. Borghesi², M H Chen¹, R.G. Evans⁶, R.R. Freeman⁵, S P Hatchett¹, J M Hill⁵, A Heron⁹, J.A. King¹, K L Lancaster², A.J. MacKinnon¹, P.A. Norreys², T Phillips¹, L. Romagnani⁷, R Snavely¹, R. Stephens⁴, C. Stoeckl⁸, R. Town¹, B Zhang³, M. Zepf⁷

¹University of California, Lawrence Livermore National Laboratory, Livermore Ca 94550, USA

²Rutherford Appleton Laboratory, Chilton, Oxon, OX110QX, United Kingdom

³University of California, Davis, Department of Applied Science, Livermore, CA 94550, USA

⁴General Atomics, San Diego, CA, USA 92186, USA

⁵The Ohio State University, Columbus, Ohio. 34210, USA

⁶Blackett Laboratory, Imperial College of Science Technology and Medicine, London SW7 2BZ, UK

⁷Depent of Pure and Applied Physics, Queens University of Belfast, Belfast BT7 1NN, UK

⁸Laboratory for Laser Energetics, University of Rochester, Rochester, NY, 14623, USA

⁹Centre de Physique Théorique (UPR14 du CNRS), Ecole Polytechnique, 91128 Palaiseau Cedex, France

Abstract

An integrated experiment relevant to fast ignition is described. A Cu doped CD spherical shell target is imploded around an inserted hollow Au cone by a six beam 600J, 1ns laser to a peak density of 4gcm^{-3} and a diameter of $100\mu\text{m}$. A 10 ps, 20TW laser pulse is focused into the cone at the time of peak compression. The flux of high-energy electrons through the imploded material is determined from the yield of Cu K α fluorescence by comparison with a Monte Carlo model and is estimated to carry 15% of the laser energy. Collisional and Ohmic heating are modeled. An electron spectrometer shows significantly greater reduction of the transmitted electron flux than is due to binary collisions and Ohmic potential. Enhanced scattering by instability-induced magnetic fields is suggested.

PACS numbers: 52.50.Jm, 52.38.Ph, 52.70.Kz

Fast ignition (FI) of inertial confined fusion ¹ is of worldwide interest because it may lead to higher gain, reduced ignition threshold, less stringent driver uniformity and target smoothness requirements and thus better prospects for inertial fusion energy ². The first integrated experiments demonstrated more than 20% efficient coupling of 1 ps pulse laser energy to a long pulse laser imploded plasma using first 60 J ^{3,4} and then 350J ⁵ pulses.

Modeling ⁶ shows that at least 14kJ of particle energy is required to ignite compressed DT plasma at a density of 300gcm^{-3} . The experimental 20% coupling efficiency implies that at approximately 70kJ laser energy would be needed. In order to generate the required 1 to 2 MeV electron energy in less than the 33 μm ignition hot spot diameter, the laser pulse must have an appropriate intensity. Constraining the intensity leads to a pulse duration close to the inertial confinement time limit of 10 to 20 ps and significantly longer than used to date ^{3,5}. We report the first integrated experiment using 10ps pulses.

The electron flux through the implosion was measured from Cu K α fluorescence induced

from Cu atoms doping of the CD shell. This method gives the greatest yield of K α where the density is highest.

Six orthogonal beams from the Vulcan laser ⁸ drove the implosion. They had jitter free synchronization with a chirped pulse amplification (CPA) short pulse, both long and short pulses being derived from the same seed pulse. The implosion drive was 0.9kJ in 1ns at 1.05 μm wavelength, with an approximately Gaussian pulse shape. The beams were focused with f/2.5 lenses with the marginal rays tangential on the micro-balloon targets. These were spherical CD shells doped at 0.7 atomic % with Cu and typically 486 μm in diameter and 6 μm thick. An Au cone inserted in the shell was 10 μm thick at its tip, which had a 30 μm flat end, located 40 μm from the center of the shell. The tapered Au thickness increased to 40 μm at the wall of the shell. The cone length was 1mm with an exterior full angle of 44° and an interior full angle of 26°.

Diagnostics included a single hit CCD spectrometer recording Cu K α , a monochromatic spherical crystal imager of Cu K α and an

electron spectrometer. The experimental configuration is described more fully elsewhere together with detailed characterization of the implosions by ps pulse Ti K α radiography⁹ and multi-MeV proton radiography¹⁰.

X-ray pinhole camera images showed good drive irradiation symmetry. The absence of detectable imploded core x-ray emission or D-D fusion neutron emission indicated a cool implosion. The measured key implosion parameters were time of peak compression 3.2 ns after the peak of the drive pulse, compressed plasma diameter 100 μm , peak density, 4 gcm^{-3} and densityx radius product, 20 mgcm^{-2} .

The average short pulse energy on target was 70 J with a peak intensity of $3 \times 10^{18} \text{ Wcm}^{-2}$. From focal spot images, half the power was delivered at a vacuum intensity less than 0.1x the peak intensity. The temperature of the source of electrons at critical density is expected to be similar to the 400 keV ponderomotive potential. There was an ASE pre-pulse with 10^{-4} of the main pulse energy and 3×10^{-7} of the intensity for a few ns prior to the main pulse. This created a sub-critical density plasma with a scale length at critical density of about 3 μm inferred from 2D hydro modeling. Self-focusing in the preformed plasma can enhance the laser intensity and sub-critical density electron acceleration processes generate electrons with temperatures higher than the ponderomotive energy, producing a higher temperature tail on the energy spectrum. The cone can also guide and concentrate both laser energy and electrons at its tip¹¹. These factors together determine the characteristics of the electron source.

Electron energy spectra along the axis of the CPA beam were obtained with a magnetic deflection spectrometer using image plate detection⁹. Spectra are shown in figure 2. The temperature of the spectrum is about 1.3 MeV in the 2 to 6 MeV range for free-standing cone. The energy spectrum of electrons escaping into vacuum is related to that of the generated electrons in an indirect fashion. Only a few percent of the total number of electrons escape, the rest being trapped by formation of a Debye sheath at the target surface. Escaping electrons lose energy to the sheath potential. The sheath potential also varies in time. For a fixed sheath potential and a Boltzmann energy spectrum, the escaping electrons have the same temperature as the source electrons. For a two-temperature distribution the sheath potential traps the lower energy electrons so that escaping electrons appear to have a higher temperature. As

discussed earlier we expect a multi- temperature distribution with the higher energies having higher temperature, consequently the 1.2 MeV slope temperature of the energy spectrum in figure 2 is not inconsistent with $3 \times 10^{18} \text{ Wcm}^{-2}$ peak intensity of the irradiation.

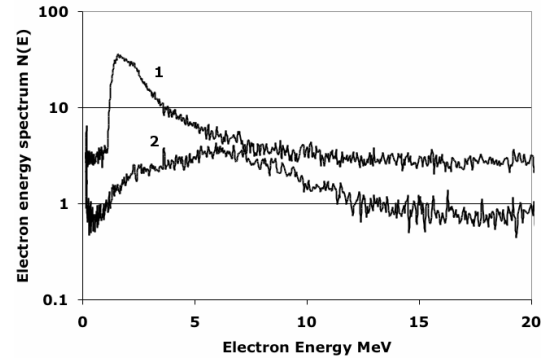


Figure 2 Electron energy spectra from a free-standing cone (1) and via an implosion (2)

The yield of Cu K α fluorescence was measured with a single hit CCD spectrometer, (Spectral Instruments x-ray CCD camera with a 2000x3200 pixel back-thinned CCD chip with a pixel size of 13 μm recorded with 16-bit resolution) from the rear of the target at an angle of 27° relative to the CPA beam. The absolute yield was determined from knowledge of the quantum efficiency, the subtended solid angle and the filter transmission¹².

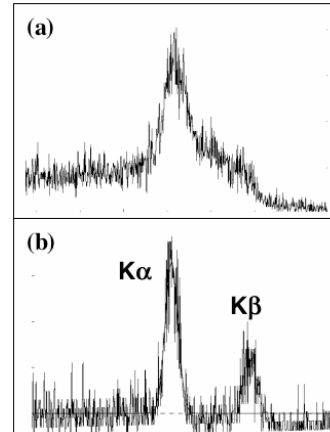


Figure 3. (a) The single hit CCD Cu K shell fluorescence spectrum from an imploded shell and (b) from a Cu foil at low energy.

Data in figure 3 show the spectrum from a 20- μm thick Cu foil irradiated at low energy (20J) exhibiting the expected ratio of K α and K β for cold Cu K shell fluorescence. The spectrum from

a full energy coned target implosion with the short pulse timed to coincide with peak compression is also shown in figure 3. The absence of $K\beta$ is attributed to thermal ionization of M shell electrons in Cu. Monte Carlo Dirac Fock (MCDF) calculations¹³ were used to compute how $K\beta$ is reduced in intensity relative to $K\alpha$, shifted to higher energy and broadened with increasing ionization. The peak velocity of the implosion of 9×10^6 cms⁻¹⁹ implies temperature at stagnation of 75eV and this causes ionization to Cu⁹⁺. The MCDF calculations indicate that for Cu⁹⁺, the $K\beta$ line is suppressed by an order of magnitude. Relevant also is that ionization effects shift and strongly broaden the $K\alpha$ line relative to the 2eV Cu $K\alpha$ spherical Bragg crystal imager bandwidth as discussed later. The maximum measured yield from an implosion was 1.1×10^{11} $K\alpha$ photons per steradian.

Null tests were conducted with long pulse ablation only of the Cu doped CD micro-balloon and no detectable $K\alpha$ yield was observed with the CCD spectrometer. Imaging with the Bragg crystal imager¹⁴ showed only extremely weak Cu $K\alpha$ emission from the ablation region with sparse single hits⁹. Cross calibration with the CCD spectrometer showed that this corresponded to <2% of the signal recorded by the CCD spectrometer. The Bragg crystal imager also showed no emission from the implosion core and this is consistent with the low efficiency of imaging the shifted and broadened $K\alpha$ emission spectrum for 75 eV temperature. We conclude that the spectrum in figure 3 is emitted from the imploded plasma. This understanding is a significant change relative an earlier preliminary analysis⁹. The absence of implosion core emission in the x-ray p.h.c. image and absence of D-D thermonuclear yield put upper bounds of 250eV and 750 eV respectively on the short pulse heating of the implosion core.

To interpret these data we first used Monte Carlo modeling with ITS (the integrated Tiger series of coupled Monte Carlo Transport Codes¹⁵) with a variable assumed Boltzmann temperature in the electron source. 10^6 electrons were injected uniformly via a 30- μ m-source diameter (the tip of the cone) in a 30° cone angle (similar to experimental observations of the cone angle of electron transport we made earlier⁷), and the injection plane was located 40 μ m from the center of the density profile in figure 4. The $K\alpha$ yield was computed using the collision cross-section and the total energy in the electrons

was obtained by scaling their number to fit the experimentally measured $K\alpha$ yield. Sensitivity to changes in the assumed source area and cone angle of the electrons was found to be slight because of the rather large imploded plasma. Sensitivity to the peak density in the implosion assuming conservation of mass, was such that if the density were higher the deduced energy in the electrons would be reduced as $\rho^{-2/3}$. The greatest sensitivity was to the electron temperature as shown in figure 4 where the conversion efficiency of laser energy to energy in the electron beam is plotted as a function of the assumed source temperature.

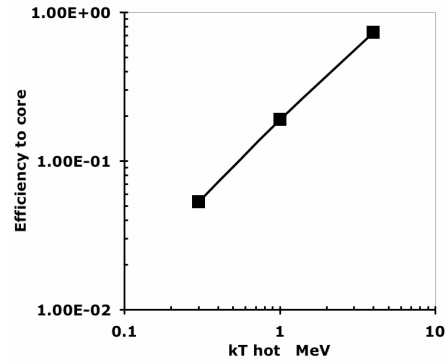


Figure 4. Conversion fraction of laser energy to energy in electrons traversing the implosion as a function of the temperature of the electrons

The source temperature as discussed previously is a distribution which has an upper bound of 1.2MeV measured by the electron spectrometer and at its low end includes the ponderomotive potential estimate of 0.4 MeV. The mean is 0.75 MeV and at this temperature figure 4, implies a conversion efficiency of 15% of the laser energy to electrons. At the extremes conversion ranges from 7% to 22%.

A model was formulated to examine the effects of Ohmic and collisional heating using as input the previously discussed 15% total energy and 0.75 MeV temperature of the electron source. The density profile of the CD and the initial temperature were those deduced from the radiography and modeling of the implosion. The geometry of the electron injection was the same as used in the MC model. Plasma resistivity has its maximum value¹⁶ at a plateau around 30 to 50 eV with decreasing resistivity at higher temperatures in the Spitzer regime at >100eV. In the model it was approximated iteratively as the value at the average temperature and density resulting from the analysis (which was 3×10^{-7} Ohm.m from the Sesame tabulation¹⁷). The

energy deposited per unit mass was calculated by injecting electrons in energy bins and calculating their Bethe Bloch collisional energy loss and Ohmic potential energy loss, stepping through axial zones along the axis of the energy transport and assuming an equal return current density. The associated collisional and Ohmic heating were also calculated, Temperature rise was approximated as that in classical plasma ionized to C^{4+} . Hydrodynamic and thermal conduction effects were neglected. Figure 5 shows the results.

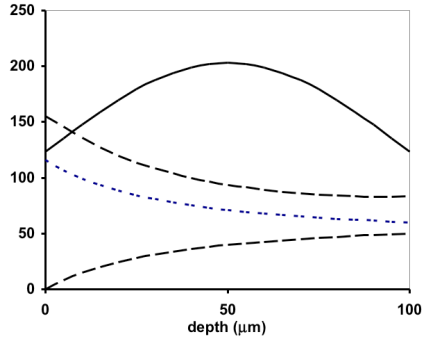


Figure 5 Heating model: solid line, density ($\times 50$) gcm^{-3} , lower dashed line, Ohmic potential ($\times 5$) keV, upper dashed line, temperature eV. Dot-dash line, temperature with no ohmic heating eV.

The temperature maximum was 155 eV located at the entry plane. It is well below the upper bounds from the x-ray phc and neutron data. The combined Ohmic and collisional heating is greatest at the entry plane because there the electron flux density is highest and the density is lowest. Ohmic heating contributes only modestly to the temperature rise as evidenced by the plot in figure 5 with no Ohmic heating. The 10 keV maximum potential is significantly smaller than the 750 keV electron temperature. The relatively small range of deduced temperatures in figure 4 makes the approximation of constant resistivity adequate for the estimates made here. The fraction of the injected electron energy absorbed in the target is 8%, a low value consistent with the small mass per unit area and small Ohmic potential.

The electron spectrometer showed in figure 4, that when the imploded plasma was present there was at least an order of magnitude reduction in the electron signal in the range 2 to 5 MeV. In most shots there was a 2 order of magnitude reduction to an un-detectable level. These data imply either enhanced energy loss or strong scattering. Electron spectrometer data from Kodama et al⁴ showed a similar but less pronounced reduction. Both effects may be

connected with strong excitation of Weibel-like and two stream instabilities with associated turbulent magnetic fields. 2D particle in cell (PIC) modeling has shown that the resulting B fields can strongly scatter the fast electrons¹⁸. They can also create a transport barrier by scattering of the return current generating an anomalous resistivity and large Ohmic potential¹⁹. Assuming a 100 fold enhanced resistivity in the heating model resulted in stopping the penetration of most of the electrons but raised the temperature in the entry region above 3 keV to a level inconsistent with the absence of thermonuclear neutron and x-ray emission from the heated implosion. Enhanced scattering is a more plausible explanation. We estimate from linear analysis²⁰ a growth exponent of 200 for the Weibel-like instability where the electron beam enters the CD plasma and 2D PIC numerical modeling¹⁸ for similar injected beam conditions shows strong scattering of the fast electrons. This could be an important issue for fast ignition needing further study.

In conclusion we have made the first measurement of electron energy transport via an imploded plasma in a fast ignition cone inserted target using a 10 ps pulse duration similar to that required for full scale experiments. We have developed a new $K\alpha$ fluorescence diagnostic to determine the efficiency of converting laser energy to electron energy injected into an implosion. Our results suggest that about 15% of the laser energy is converted to electron energy traversing the implosion. The data also show attenuation of the electron flux density recorded in vacuum, which is best explained by scattering from instability generated B fields.

Acknowledgements. We are grateful to the staff of the Central laser facility, in particular J. Collier, S. Hawkes, R. Heathcote, C. Hernandez-Gomez, D. Neely and M.H.R. Hutchinson for their support. Work performed under the auspices of the U.S. Department of Energy by the Lawrence Livermore National Laboratory under Contract No. W-7405-ENG-48.

¹ N.G. Basov, S.Y. Guskov and L.P. Feokistov, *J. Sov. Laser Res.* **13**, 396 (1992). and M Tabak et al *Phys Plasmas* **1** 1626 (1994)

² M H Key et al *J Fusion Energy* **17**, 231 (1998)

³ R Kodama et al *Nature* **412**, 798 (2001)

⁴ M H Key *Nature* **412**, 775 (2001)

⁵ R K Kodama et al. *Nature* **418**, 933 (2002)

⁶ S Atzeni *Phys Plasmas* **6** 3317 (1999)

-
- ⁷ R.B. Stephens et al. Phys. Rev E. 69, (2004)
- ⁸ C. N. Danson et al J. Mod. Opt. **45**, 1653 (1998)
- ⁹ P Norreys et al Phys Plasmas .11,2746, (2004) and J A King et al Appl. Phys. Lett. 86,191501, (2005).
- ¹⁰ A J MacKinnon et al Rev Sci Instr. 75, 3531, 2004) and Phys Rev. Lett.(in press)
- ¹¹ Y Sentoku et al Phys Rev E 11, 3083,(2004)
- ¹² C. Stoeckl et al., Rev. Sci. Instrum. **75**, 3705,(2004).
- ¹³ M. H. Chen, Phys. Rev. A 31, 1449 (1985)
- ¹⁴ J. A. Koch *et al.*, Rev. Sci. Instrum. **74**, 2130 (2003).
- ¹⁵ J A Halbeib and T A Melhorn. Sandia National Laboratory Report #SAND84-0573 (1984)
- ¹⁶ H. M. Milchberg *et al.*, Phys. Rev. Lett. **62**, 2364 (1988) and Y. T. Lee and R. M. More, Physics of Fluids 27, 1273 (1984)
- ¹⁷ S P Lyon and J D Johnson. Los Alamos National Lab Report LA-UR-92-3407(1992)
- ¹⁸ J C Adam et.al. to be published
- ¹⁹ Y Sentoku et al. Phys Rev Lett.90,155001(2003)
- ²⁰ J M Hill et al. Phys Plasmas (accepted for publication)